ECCOMAS
Proceedia

GENERALIZED MACROELEMENT FOR GEOMETRICALLY AND MATERIALLY NON-LINEAR ANALYSIS OF STEEL MEMBERS

Konstantinos E. Morfidis[1]

[1] Assistant Researcher, Earthquake Planning and Protection Organization (EPPO-ITSAK)
Terma Dasylliou, 55535, Thessaloniki, Greece
e-mail: konmorf@gmail.com

Abstract

The demand for a reliable modelling of steel structures introduces the need for the implementation of advanced techniques. Due to the shape and the properties of steel members, as well as the connections among them, the performance of materially and geometrically non-linear analyses are required in order to approach effectively the actual behavior of the steel structures. To this end, special calculation tools must be available in the software which is used for analysis and design. More specifically, phenomena such as the bending, the torsional and the torsional-flexural buckling as regards the geometric non-linear effects, and the elasto-plastic behavior of steel in critical cross-sections, as regards the materially non-linear effects, require the implementation of appropriate stiffness matrices and load vectors. These calculation tools are available in the literature. However, the inclusion of all required features in a finite element demands a specific formulation. Therefore, the purpose of the present paper is to propose the formulation of a two-noded macroelement with seven degrees of freedom per node, which possesses abilities to model effectively the above-mentioned phenomena in practice. On the basis of a two-stage static condensation technique, the proposed finite element includes features appropriate for the modelling of material non-linearity effects and the semi-rigid connections (through non-linear rotational springs), as well as the modelling of the geometric non-linear effects (using appropriate finite element formulation), and the influence of the rigid joints (through rigid offsets). The proposed macroelement was successfully added to the finite elements' library of an existing professional software for the analysis and design of steel structures. The reliability of the proposed element is tested in the current paper using the solutions of well-known problems selected from the literature.

Keywords: Steel structures, Finite Element Method, Nonlinear Analysis, Buckling, Beam/Column elements.

1 INTRODUCTION

The analysis and design of members of steel structures require the implementation of specific modelling techniques (see e.g. [1-3]). The requirement of these techniques arises from the fact that the shape and the load conditions of steel beams and columns make them sensitive to the consequences of phenomena which are related with geometric and material nonlinearities. Such phenomena are, for example the bending buckling, the torsional and torsional-flexural buckling as regards the geometric non-linear effects, and the elasto-plastic behavior of steel in critical cross-sections, as regards the materially non-linear effects. The existence of these unfavorable influences on the steel members has been recognized by the former, as well as by the modern, seismic codes, e.g. [4, 5]. Thus, the problem of the effective design of steel structures against static or dynamic (e.g. seismic) loads is treated in the cross-section and member levels. For this reason, specific recommendations are proposed which, however, require the appropriate (and most accurate possible) modelling. A significant number of research studies (e.g. [6-10]) and scientific books (e.g. [11-13]) focused on the effective modelling of steel members have been published. The existing theories regarding the elasto-plastic behavior of steel, as well as the continuous improvement of finite element formulation in combination with the computational abilities of the modern hardware, offer the possibility of a more effective approach to the behavior of steel structural members.

In the current paper, the formulation of a new two-noded macroelement with seven degrees of freedom per node, which can effectively model steel structures members in practice, is presented. Based on a two-stage static condensation technique, the proposed formulation includes features appropriate for the modelling of material non-linearity effects and the semi-rigid connections (through non-linear rotational springs), the modelling of the geometric non-linear effects (using appropriate finite element formulation), and the influence of the rigid joints (through rigid offsets). Using the static condensation method, the proposed element, with 14 degrees of freedom, can be compatible with the classic two-noded elements (with 12 degrees of freedom) and co-exist with them in structures' models. Thus, the problem of the design of steel members in the cross-section and member levels can be handled practically using a compact formulation. The reliability of the proposed element is tested using the solutions of well-known problems selected from the literature.

2 FORMULATION OF THE PROPOSED MACROELEMENT

2.1 General description of the element

The proposed macroelement consists of three segments, as shown in Figure 1. More specifically:

- the end segment between the external node 1 and the internal (virtual) node 2, and the corresponding end segment between the internal (virtual) node 3 and the external node 4. In each one of these segments, three absolutely rigid rod elements (perpendicular between them) are defined. These elements are the three spatial components of the end rigid offsets (in the local coordinate system of the macroelement) which model the bodies of beam-to-column joints.
- the median segment between the internal nodes 2 and 3. This segment models the flexible part of the macroelement. The type of finite element which is used in this segment can be selected on the basis of the considered problem. For example, Bernoulli or Timoshenko beam elements can be used (see eg. [14]). In the present paper, the formulation which is used for the modelling of the median segment will be described in the following sections.

The connection of the median segment to the rigid offsets is achieved by means of rotational springs. These springs can be considered either as linear for (1st or 2nd order) elastic analyses, or as nonlinear (in conjunction with M-φ diagrams) for materially non-linear analyses in the framework of the concentrated plasticity model.
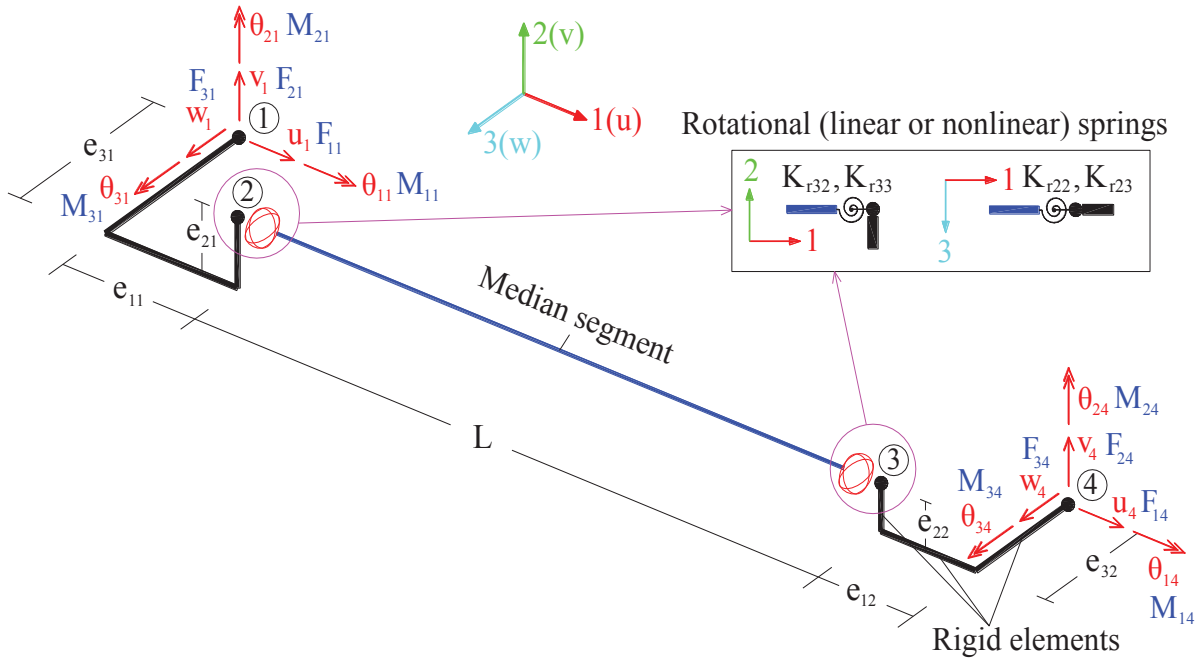

Figure 1: General description of the proposed macroelement

In Figure 1, the degrees of freedom (d.o.f.) of the proposed macroelement are also illustrated. It can be seen that they are 12 in number, as in case of the classic beam/column elements. The 7th d.o.f., which is required for the modelling of the effect of warping, is considered only in the median segment. Thus, the median segment can be an element with 14 d.o.f. The procedure of the transformation of the 14 d.o.f. of the median segment to the 12 d.o.f. of the whole macroelement will be described in sections 2.2 and 2.3.

2.2 Stiffness matrix derivation

The stiffness matrix of the macroelement is derived in two steps. In the first step, the stiffness matrix of the median segment's element is formed. In the second step, the matrix relation between the stiffness matrix of the median segment and the stiffness matrix of the macroelement is formulated. This relation demonstrates the effect of the rotational springs and the rigid offsets on the stiffness matrix of the macroelement.

A) Step 1: Derivation of the stiffness matrix for the median segment

The method for the derivation of the stiffness matrix of the median segment's element is based on the static condensation procedure (e.g. [15,16]). In general, static condensation is used in order to reduce the number of the equations which constitute the system of equations of equilibrium. In the present case, static condensation is necessary due to the fact that the stiffness matrix of the median segment is based on the approach of the displacement field through algebraic interpolation functions. These functions are used when the 7th d.o.f. must be considered for the modelling of the warping effect, because, in this case, the exact solution of the corresponding differential equations of equilibrium is not available. Thus, the discretization of the median segment is necessary. This discretization causes the increase of the nodes and, consequently, the increase of the d.o.f. of the macroelement. Moreover, when the 7th d.o.f.

is considered, the corresponding elements' stiffness matrices are 14x14 matrices, not compatible with the classic 12x12 stiffness matrices which are mainly used in practice.

For this reason, in the present paper, the implementation of the static condensation procedure in two stages is proposed (Figure 2). In the first stage, all the internal d.o.f., which arise from the discretization of the median segment's element, are condensed. Thus, if the number of the sub-elements in which the median segment is discretized is **n** (using **n**+1 nodes: **n**-1 internal and 2 external), then the corresponding stiffness matrix is a $[7(\mathbf{n}+1)]\times[7(\mathbf{n}+1)]$ matrix.
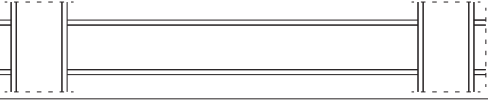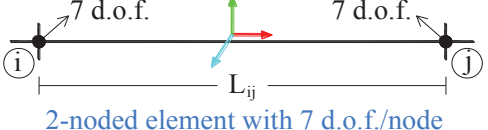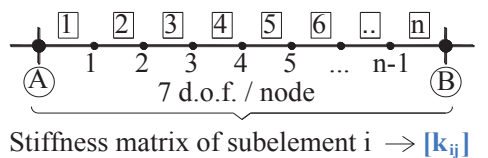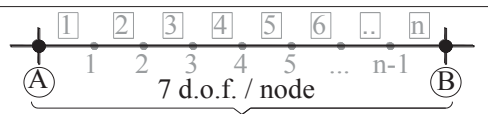
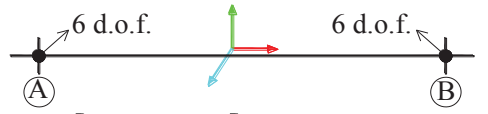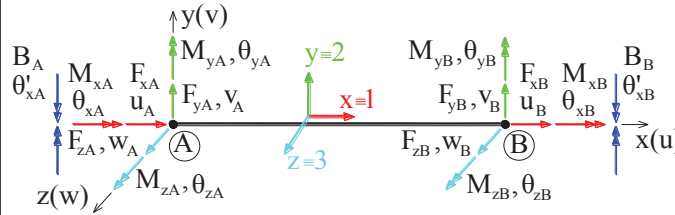| STEP	DESCRIPTION	COMMENTS
Actual member	*(figure: steel beam member)*	Beam, member of a steel structure (e.g. steel frame)
First step: Definition of the stiffness matrix for the subelements of the median segment	*(figure: 2-noded element, 7 d.o.f. at each node i and j, length L_{ij})* 2-noded element with 7 d.o.f./node	Stiffness matrix: $[\mathbf{k_{ij}}]$ (14x14)
Second step: Discretization of the median segment in **n** subelements (**n**-1 internal nodes, 2 external nodes: A,B)	*(figure: subelements 1,2,3,4,5,6,..,n with nodes A,1,2,3,4,5,...,n-1,B)* 7 d.o.f. / node. Stiffness matrix of subelement i $\rightarrow [\mathbf{k_{ij}}]$	Formation of a "sub-structure" consisting of **n** subelements: $\rightarrow$ Stiffness matrix: $[\mathbf{k_{sub}}]\ [7(\mathbf{n}+1)\times 7(\mathbf{n}+1)]$ $\rightarrow$ Load matrix: $[\mathbf{p_{sub}}]\ [7(\mathbf{n}+1)\times 1]$
Third step: First stage of static condensation $\rightarrow$ Condensation of d.o.f of the internal nodes $\downarrow$ Generation of 2-noded macroelement with 7 d.o.f. / node	*(figure of nodes A,B)* 7 d.o.f. / node $$[\mathbf{k_{sub}}]=\begin{bmatrix}[\mathbf{k_{sub}^{(AB-AB)}}] & [\mathbf{k_{sub}^{(AB-int)}}]\\ 14\times14 & 14\times7(\mathbf{n}\text{-}1)\\ [\mathbf{k_{sub}^{(int-AB)}}] & [\mathbf{k_{sub}^{(int-int)}}]\\ 7(\mathbf{n}\text{-}1)\times14 & 7(\mathbf{n}\text{-}1)\times7(\mathbf{n}\text{-}1)\end{bmatrix}$$ d.o.f. of the nodes A, B / d.o.f. of the internal nodes $$[\mathbf{p_{sub}}]^T=\begin{bmatrix}[\mathbf{p_{sub}^{(AB-AB)}}] & [\mathbf{p_{sub}^{(int-AB)}}]\\ 14\times1 & 7(\mathbf{n}\text{-}1)\times1\end{bmatrix}$$	Generation of: Stiffness matrix $[\mathbf{k_{s.c.1}}]$ (14x14) Load matrix $[\mathbf{p_{s.c.1}}]$ (14x1) $\rightarrow$ Equation of Equilibrium: $[\mathbf{k_{s.c.1}}]\cdot[\mathbf{u_{s.c.1}}]+[\mathbf{p_{s.c.1}}]=[\mathbf{F_{s.c.1}}]$ $[\mathbf{u_{s.c.1}}]$= the (14x1) vector of the displacements of nodes A,B (includes and the warping d.o.f.) $[\mathbf{F_{s.c.1}}]$= the (14x1) vector of the forces of nodes A, B
Fourth step: Second stage of static condensation $\rightarrow$ Condensation of the warping d.o.f. in nodes A, B $\downarrow$ Generation of 2-noded macroelement with the conventional 6 d.o.f. in each of nodes A, B	*(figure: 6 d.o.f. at nodes A, B)* $$[\mathbf{k_{s.c.1}}]=\begin{bmatrix}[\mathbf{k_{s.c.1}^{(cc)}}] & [\mathbf{k_{s.c.1}^{(cn)}}]\\ 12\times12 & 12\times2\\ [\mathbf{k_{s.c.1}^{(nc)}}] & [\mathbf{k_{s.c.1}^{(nn)}}]\\ 2\times12 & 2\times2\end{bmatrix}$$ conventional d.o.f. of the nodes A, B / warping d.o.f. of the nodes A, B $$[\mathbf{p_{s.c.1}}]^T=\begin{bmatrix}[\mathbf{p_{s.c.1}^{(cc)}}] & [\mathbf{p_{s.c.1}^{(nc)}}]\\ 12\times1 & 2\times1\end{bmatrix}\quad [\mathbf{F_{s.c.1}}]^T=\begin{bmatrix}[\mathbf{F_{s.c.1}^{(cc)}}] & [\mathbf{F_{s.c.1}^{(nc)}}]\\ 12\times1 & 2\times1\end{bmatrix}$$	Generation of matrices for the median segment $[\mathbf{k_{ms}}]$ (12x12) and $[\mathbf{p_{ms}}]$ (12x1) $\rightarrow$ Equation of Equilibrium of the median segment: $[\mathbf{k_{ms}}]\cdot[\mathbf{u_{ms}}]+[\mathbf{p_{ms}}]=[\mathbf{F_{ms}}]$ $[\mathbf{u_{ms}}]$= the (12x1) vector of the displacements of nodes A, B $[\mathbf{F_{ms}}]$= the (12x1) vector of the forces of nodes A, B

(bottom figure: coordinate system with axes y(v) [y≡2], x(u) [x≡1], z(w) [z≡3], showing node A with $B_A, \theta'_{xA}, M_{xA}, F_{xA}, \theta_{xA}, u_A, M_{yA}, \theta_{yA}, F_{yA}, v_A, F_{zA}, w_A, M_{zA}, \theta_{zA}$ and node B with $M_{yB}, \theta_{yB}, F_{xB}, M_{xB}, B_B, \theta'_{xB}, F_{yB}, v_B, u_B, \theta_{xB}, F_{zB}, w_B, M_{zB}, \theta_{zB}$)

$$[\mathbf{u_{s.c.1}}]^T=[u_A\ v_A\ w_A\ \theta_{xA}\ \theta_{yA}\ \theta_{zA}\ u_B\ v_B\ w_B\ \theta_{xB}\ \theta_{yB}\ \theta_{zB}\ \theta'_{xA}\ \theta'_{xB}]$$

$$[\mathbf{F_{s.c.1}}]^T=[F_{xA}\ F_{yA}\ F_{zA}\ M_{xA}\ M_{yA}\ M_{zA}\ F_{xB}\ F_{yB}\ F_{zB}\ M_{xB}\ M_{yB}\ M_{zB}\ B_A\ B_B]$$

$$[\mathbf{p_{s.c.1}}]^T=[p_{xA}\ p_{yA}\ p_{zA}\ m_{xA}\ m_{yA}\ m_{zA}\ p_{xB}\ p_{yB}\ p_{zB}\ m_{xB}\ m_{yB}\ m_{zB}\ b_A\ b_B]$$

Figure 2: The steps of the two-stage static condensation procedure

Eliminating all the internal nodes at the first stage of the procedure, the $[7(\mathbf{n}+1)]\times[7(\mathbf{n}+1)]$ stiffness matrix is transformed to a 14x14 matrix. Then, at the second stage of the procedure, the 7th d.o.f. which corresponds to warping is condensed, transforming the 14x14 stiffness matrix $[\mathbf{k_{s.c.1}}]$ to a 12x12 stiffness matrix $[\mathbf{k_{ms}}]$ for the median segment (Figure 2).

As regards the matrix transformations which are required for the static condensation in each one of the two stages, it must be noted that, whereas the first one of them is always performed using a specific procedure, the second one depends on the boundary conditions which concern the warping effects in the end nodes of the median segment. Thus, the stiffness matrix $[\mathbf{k_{s.c.1}}]$ and the load matrix $[\mathbf{p_{s.c.1}}]$ of the median segment after the first stage of the static condensation (Figure 2) are given by Eq. (1), (e.g. [17]):

$$\left[k_{s.c.1} \right] = \left[k_{sub}^{(AB-AB)} \right] - \left[k_{sub}^{(AB-int)} \right] \cdot \left[k_{sub}^{(int-int)} \right]^{-1} \cdot \left[k_{sub}^{(int-AB)} \right]$$

$$\left[p_{s.c.1} \right] = \left[p_{sub}^{(AB-AB)} \right] - \left[k_{sub}^{(AB-int)} \right] \cdot \left[k_{sub}^{(int-int)} \right]^{-1} \cdot \left[p_{sub}^{(int-AB)} \right]$$

(1)

The required matrix transformations for the second stage of the static condensation are summarized in Table 1.

Case	Boundary condition in node A	Boundary condition in node B	Condensed stiffness matrix $[\mathbf{k_{ms}}]$	Condensed load matrix $[\mathbf{p_{ms}}]$
1	Bimoment $B_A=0$	Bimoment $B_B=0$	$\left[k_{s.c.1}^{(cc)} \right] - \left[k_{s.c.1}^{(cn)} \right] \cdot \left[k_{s.c.1}^{(nn)} \right]^{-1} \cdot \left[k_{s.c.1}^{(nc)} \right]$	$\left[p_{s.c.1}^{(cc)} \right] - \left[k_{s.c.1}^{(cn)} \right] \cdot \left[k_{s.c.1}^{(nn)} \right]^{-1} \cdot \left[p_{s.c.1}^{(nc)} \right]$
2	$\theta'_{XA}=0$	$\theta'_{XB}=0$	$\left[k_{s.c.1}^{(cc)} \right]$	$\left[p_{s.c.1}^{(cc)} \right]$
3	Bimoment $B_A=-s_A\theta'_{XA}$	Bimoment $B_B=-s_B\theta'_{XB}$	As in case 1, with: $\left[\bar{k}_{s.c.1}^{(nn)} \right] = \left[k_{s.c.1}^{(nn)} \right] + \begin{bmatrix} s_A & 0 \\ 0 & s_B \end{bmatrix}$	
4	$B_A=0$	$B_B=-s_B\theta'_{XB}$	As in case 3, with: $\left[\bar{k}_{s.c.1}^{(nn)} \right] = \left[k_{s.c.1}^{(nn)} \right] + \begin{bmatrix} 0 & 0 \\ 0 & s_B \end{bmatrix}$	
5	Bimoment $B_A=0$	Warping $\theta'_{XB}=0$	$\left[k_{s.c.1}^{(cc)} \right] - \dfrac{1}{k_{s.c.1}^{(nnAA)}} \cdot \left[k_{s.c.1}^{(cnA)} \right] \cdot \left[k_{s.c.1}^{(ncA)} \right]$	$\left[p_{s.c.1}^{(cc)} \right] - \dfrac{1}{k_{s.c.1}^{(nnAA)}} \cdot \left[k_{s.c.1}^{(cnA)} \right] \cdot b_A$
6	$\theta'_{XA}=0$	$B_B=-s_B\theta'_{XB}$	$\left[k_{s.c.1}^{(cc)} \right] - \dfrac{1}{k_{s.c.1}^{(nnBB)}+s_B} \cdot \left[k_{s.c.1}^{(cnB)} \right] \cdot \left[k_{s.c.1}^{(ncB)} \right]$	$\left[p_{s.c.1}^{(cc)} \right] - \dfrac{b_B}{k_{s.c.1}^{(nnBB)}+s_B} \cdot \left[k_{s.c.1}^{(cnB)} \right]$

Table 1: Summary of matrix transformations in the second stage of the static condensation

Where:

$\left[k_{s.c.1}^{(cc)} \right], \left[k_{s.c.1}^{(cn)} \right], \left[k_{s.c.1}^{(nn)} \right], \left[k_{s.c.1}^{(nc)} \right]$ are sub-matrices of $\left[k_{s.c.1} \right]$ after the first stage of the static condensation (Figure 2),

$\left[p_{s.c.1}^{(cc)} \right], \left[p_{s.c.1}^{(nc)} \right]$ are sub-matrices of $\left[p_{s.c.1} \right]$ after the first stage of the static condensation (Figure 2),

$\left[k_{s.c.1}^{(cnA)} \right], \left[k_{s.c.1}^{(ncA)} \right], \left[k_{s.c.1}^{(cnB)} \right], \left[k_{s.c.1}^{(ncB)} \right]$ are sub-matrices and $k_{s.c.1}^{(nnAA)}$, $k_{s.c.1}^{(nnBB)}$ are elements of $\left[k_{s.c.1} \right]$, if this matrix is written in the following expanded form:

$$\left[k_{s.c.1} \right] = \begin{bmatrix} \left[k_{s.c.1}^{(cc)} \right] & \left[k_{s.c.1}^{(cnA)} \right] & \left[k_{s.c.1}^{(cnB)} \right] \\ \left[k_{s.c.1}^{(ncA)} \right] & k_{s.c.1}^{(nnAA)} & k_{s.c.1}^{(nnAB)} \\ \left[k_{s.c.1}^{(ncB)} \right] & k_{s.c.1}^{(nnBA)} & k_{s.c.1}^{(nnBB)} \end{bmatrix}$$

It must be noted that cases 3 and 4 in Table 1 correspond to the partial restraint of warping in end nodes A, B (for details see e.g. [18]). Thus, s_A, s_B are the constants of the warping spring elements which partially restrain the warping. Finally, the terms b_A, b_B (see Figure 2) are elements of the median segment's load matrix **[p$_{s.c.1}$]**, which correspond to the warping d.o.f. in the end nodes A, B.

The procedure described in Figure 2 is based on the derivation of the stiffness matrices **[k$_{ij}$]** for the sub-elements (ij) which are the basic components of the macroelement (see the first step of the procedure in Figure 2). The stiffness matrices for these sub-elements are available in the literature (see e.g. [6, 7]). Their formulation is based on the linearized updated Lagrangian formulation of the equation of the incremental virtual work for a beam/column element which possesses 7 d.o.f. in the end nodes (Eq. (2)):

$$\frac{1}{2}\int_0^{L_{ij}}\left[EA\delta\left(\frac{du}{dx}\right)^2+EI_{yy}\delta\left(\frac{d^2w}{dx^2}\right)^2+EI_{zz}\delta\left(\frac{d^2v}{dx^2}\right)^2+EC_\omega\delta\left(\frac{d^2\theta_x}{dx^2}\right)^2+GJ\left(\frac{d\theta_x}{dx}\right)^2\right]dx+$$

$$+\frac{1}{2}\int_0^{L_{ij}}F_x\delta\left[\left(\frac{dv}{dx}\right)^2+\left(\frac{dw}{dx}\right)^2\right]dx+\int_0^{L_{ij}}\frac{K_w}{2}\delta\left(\frac{d\theta_x}{dx}\right)^2dx-\int_0^{L_{ij}}\left[V_y\delta\left(\frac{du}{dx}\frac{dv}{dx}\right)+V_z\delta\left(\frac{du}{dx}\frac{dw}{dx}\right)\right]dx-$$

$$-\int_0^{L_{ij}}M_y\delta\left(\frac{dv}{dx}\frac{d\theta_x}{dx}\right)dx-\int_0^{L_{ij}}M_z\delta\left(\frac{dw}{dx}\frac{d\theta_x}{dx}\right)dx-\frac{1}{2}\int_0^{L_{ij}}M_x\left[\delta\left(\frac{dv}{dx}\frac{d^2w}{dx^2}\right)-\delta\left(\frac{d^2v}{dx^2}\frac{dw}{dx}\right)\right]dx+ \tag{2}$$

$$+\int_0^{L_{ij}}V_y\delta\left(\frac{dw}{dx}\theta_x\right)dx-\int_0^{L_{ij}}V_z\delta\left(\frac{dv}{dx}\theta_x\right)dx=\{\delta u\}^T\left(\{^2f\}-\{^1f\}\right)$$

Where: E is the modulus of elasticity; G is the shear modulus; A is the area of the beam/column's cross-section; I_{yy}, I_{zz} are the moments of inertia of the beam/column's cross-section with respect to local axes y, z (Figure 2); J is the torsional constant; C_ω is the warping constant; L_{ij} is the length of the element; $\{du\}$ is the vector of the displacements of nodes i and j (Figure 2); $\{f\}$ is the vector of forces of nodes i and j (Figure 2) and $K_w=[F_x(I_{yy}+I_{zz})]/A$ is the Wagner coefficient. It must also be noted that the right superscripts 1 and 2 of vector $\{f\}$ refer to the deformed configurations C_1 (the last known state) and C_2 (current deformed state). Both of these configurations are defined in the framework of the updated Lagrangian approach, as the start and the end of each incremental step of external loading (see e.g. [11]).

In order to derive the stiffness matrix **[k$_{ij}$]** starting from Eq. (2), the displacement field of the element (ij) must be defined. For this reason, the following shape functions are used:

$$N_1=N_1(x)=1-\left(x/L_{ij}\right) \qquad\qquad N_2=N_2(x)=\left(x/L_{ij}\right)$$

$$N_3=N_3(x)=1-3\cdot\left(x/L_{ij}\right)^2+2\cdot\left(x/L_{ij}\right)^3 \qquad N_4=N_4(x)=x-2\cdot\left(x^2/L_{ij}\right)+\left(x^3/L_{ij}^2\right) \tag{3}$$

$$N_5=N_5(x)=3\cdot\left(x/L_{ij}\right)^2-2\cdot\left(x/L_{ij}\right)^3 \qquad N_6=N_6(x)=-\left(x^2/L_{ij}\right)+\left(x^3/L_{ij}^2\right)$$

The corresponding matrices of these functions are:

$$\begin{array}{c}\qquad\quad u_A\quad v_A\quad w_A\quad \theta_{XA}\quad \theta_{YA}\quad \theta_{ZA}\quad u_B\quad v_B\quad w_B\quad \theta_{XB}\quad \theta_{YB}\quad \theta_{ZB}\;\vdots\;\theta'_{XA}\quad \theta'_{XB}\\ \left[N_u\right]=[N_1\quad 0\quad 0\quad 0\quad 0\quad 0\quad N_2\quad 0\quad 0\quad 0\quad 0\quad 0\;\vdots\;0\quad 0]\end{array}$$

$$\begin{array}{c}\qquad\quad u_A\quad v_A\quad w_A\quad \theta_{XA}\quad \theta_{YA}\quad \theta_{ZA}\quad u_B\quad v_B\quad w_B\quad \theta_{XB}\quad \theta_{YB}\quad \theta_{ZB}\;\vdots\;\theta'_{XA}\quad \theta'_{XB}\\ \left[N_v\right]=[0\quad N_3\quad 0\quad 0\quad 0\quad N_4\quad 0\quad N_5\quad 0\quad 0\quad 0\quad N_6\;\vdots\;0\quad 0]\end{array}$$

$$\begin{array}{c}\qquad\quad u_A\quad v_A\quad w_A\quad \theta_{XA}\quad \theta_{YA}\quad \theta_{ZA}\quad u_B\quad v_B\quad w_B\quad \theta_{XB}\quad \theta_{YB}\quad \theta_{ZB}\;\vdots\;\theta'_{XA}\quad \theta'_{XB}\\ \left[N_w\right]=[0\quad 0\quad N_3\quad 0\quad -N_4\quad 0\quad 0\quad 0\quad N_5\quad 0\quad -N_6\quad 0\;\vdots\;0\quad 0]\end{array} \tag{4}$$

$$\begin{array}{c}\qquad\quad u_A\quad v_A\quad w_A\quad \theta_{XA}\quad \theta_{YA}\quad \theta_{ZA}\quad u_B\quad v_B\quad w_B\quad \theta_{XB}\quad \theta_{YB}\quad \theta_{ZB}\;\vdots\;\theta'_{XA}\quad \theta'_{XB}\\ \left[N_\theta\right]=[0\quad 0\quad 0\quad N_3\quad 0\quad 0\quad 0\quad 0\quad 0\quad N_5\quad 0\quad 0\;\vdots\;N_4\quad N_6]\end{array}$$

Thus, the displacement in any point inside the element can be expressed in terms of its end nodes displacements using Eq. (5):

$$u = [N_u]\{u\} \quad v = [N_v]\{u\} \quad w = [N_w]\{u\} \quad \theta_x = [N_\theta]\{u\}$$

$$\{u\} = \begin{bmatrix} u_i & v_i & w_i & \theta_{xi} & \theta_{yi} & \theta_{zi} & u_j & v_j & w_j & \theta_{xj} & \theta_{yj} & \theta_{zj} & \theta'_{xj} & \theta'_{xj} \end{bmatrix}^T$$

(5)

Eq. (2) also introduces the internal forces of the element (ij): F_x, V_y, V_z, M_x, M_y and M_z. Assuming that no loads act on the element, these forces can be expressed in terms of the corresponding forces in the element's ends i and j, using the relations of Eq. (6):

$$F_x = F_{xj}, \quad V_y = -\frac{M_{zi} + M_{zj}}{L_{ij}}, \quad V_z = \frac{M_{yi} + M_{yj}}{L_{ij}}$$

$$M_x = M_{xj}, \quad M_y = -M_{yi}\left(1 - \frac{x}{L_{ij}}\right) + M_{yj}\left(\frac{x}{L_{ij}}\right), \quad M_z = -M_{zi}\left(1 - \frac{x}{L_{ij}}\right) + M_{zj}\left(\frac{x}{L_{ij}}\right)$$

(6)

Inserting Eqs. (5), (6) into Eq. (2), and after a specific transformation (e.g. [6, 8, 19]), the stiffness matrix of the element (ij) can be expressed as follows:

$$\begin{aligned}
\left[k_{ij}\right] = {} & EA\left[k_{uu}^{110}\right] + EI_{zz}\left[k_{vv}^{220}\right] + EI_{yy}\left[k_{ww}^{220}\right] + GJ\left[k_{\theta\theta}^{110}\right] \\
& + F_{xj}\left[k_{vv}^{110}\right] + F_{xj}\left[k_{ww}^{110}\right] + V_y\left[k_{uv}^{110}\right] + V_y\left[k_{vu}^{110}\right] \\
& - V_z\left[k_{uw}^{110}\right] - V_z\left[k_{wu}^{110}\right] + K_w\left[k_{\theta\theta}^{110}\right] - \frac{M_{yi} + M_{yj}}{L_{ij}}\left(\left[k_{v\theta}^{100}\right] + \left[k_{\theta v}^{010}\right] + \left[k_{v\theta}^{111}\right] + \left[k_{\theta v}^{111}\right]\right) \\
& + M_{yi}\left[k_{v\theta}^{110}\right] + M_{yi}\left[k_{\theta v}^{110}\right] + M_{zi}\left[k_{w\theta}^{110}\right] + M_{zi}\left[k_{\theta w}^{110}\right] \\
& - \frac{M_{xj}}{2}\left[k_{vw}^{120}\right] - \frac{M_{xj}}{2}\left[k_{wv}^{210}\right] + \frac{M_{xj}}{2}\left[k_{vw}^{210}\right] + \frac{M_{xj}}{2}\left[k_{wv}^{120}\right] \\
& - \frac{M_{zi} + M_{zj}}{L_{ij}}\left(\left[k_{w\theta}^{100}\right] + \left[k_{\theta w}^{010}\right] + \left[k_{w\theta}^{111}\right] + \left[k_{\theta w}^{111}\right]\right) + EC_\omega\left[k_{\theta\theta}^{220}\right]
\end{aligned}$$

(7)

Where:

$$\left[k_{gh}^{stv}\right] = \int_0^{L_{ij}} \frac{d^s\left[N_g\right]^T}{dx^s} \cdot \frac{d^t\left[N_h\right]}{dx^t} \cdot x^v dx$$

$$g = u, v, w \quad h = u, v, w$$
$$s, t = \text{order of differentation}$$
$$v = \text{order of exponent of } x$$

(8)

From the study of Eq. (7), it can be concluded that the stiffness matrix [k_{ij}] (which can be used for geometric non-linear analysis, additionally including the influence of the warping effects) consists of 28 matrices. These matrices correspond to contribution of the element's elastic deformations and to the contribution of the element's end forces. On the basis of the above conclusion, the stiffness matrix can expressed as the summation of two matrices: the linear elastic stiffness matrix [$k_{ij,e}$] and the geometric stiffness matrix [$k_{ij,g}$]:

$$\left[k_{ij}\right] = \left[k_{ij,e}\right] + \left[k_{ij,g}\right]$$

(9)

Where:

$$\left[k_{ij,e}\right]=EA\left[k_{uu}^{110}\right]+EI_{zz}\left[k_{vv}^{220}\right]+EI_{yy}\left[k_{ww}^{220}\right]+GJ\left[k_{\theta\theta}^{110}\right]+EC_{\omega}\left[k_{\theta\theta}^{220}\right] \quad (10a)$$

$$\left[k_{ij,g}\right]=F_{xj}\left[k_{vv}^{110}\right]+F_{xj}\left[k_{ww}^{110}\right]+V_{y}\left[k_{uv}^{110}\right]+V_{y}\left[k_{vu}^{110}\right]$$

$$-V_{z}\left[k_{uw}^{110}\right]-V_{z}\left[k_{wu}^{110}\right]+K_{w}\left[k_{\theta\theta}^{110}\right]-\frac{M_{yi}+M_{yj}}{L_{ij}}\left(\left[k_{v\theta}^{100}\right]+\left[k_{\theta v}^{010}\right]+\left[k_{v\theta}^{111}\right]+\left[k_{\theta v}^{111}\right]\right)$$

$$+M_{yi}\left[k_{v\theta}^{110}\right]+M_{yi}\left[k_{\theta v}^{110}\right]+M_{zi}\left[k_{w\theta}^{110}\right]+M_{zi}\left[k_{\theta w}^{110}\right] \quad (10b)$$

$$-\frac{M_{xj}}{2}\left[k_{vw}^{120}\right]-\frac{M_{xj}}{2}\left[k_{wv}^{210}\right]+\frac{M_{xj}}{2}\left[k_{vw}^{210}\right]+\frac{M_{xj}}{2}\left[k_{wv}^{120}\right]$$

$$-\frac{M_{zi}+M_{zj}}{L_{ij}}\left(\left[k_{w\theta}^{100}\right]+\left[k_{\theta w}^{010}\right]+\left[k_{w\theta}^{111}\right]+\left[k_{\theta w}^{111}\right]\right)$$

B) Step 2: Derivation of the stiffness matrix [k_me] for the macroelement

After the formulation of the stiffness matrix for the macroelement's median segment according to the procedure which is summarized in Figure 2, the corresponding stiffness matrix for the whole macroelement (Figure 1) can be derived.

At the beginning, the relationships between the displacements of internal nodes 2 and 3, with those of external nodes 1 and 4 (Figure 1) are established. To this end, two factors must be considered: (a) the fact that the rigid offsets are non-deformable elements and behave as absolutely rigid bodies in 3D-space, and (b) the existence of the rotational springs which are located in internal nodes 2, 3, where the median segment is connected to the rigid offsets (Figure 1).
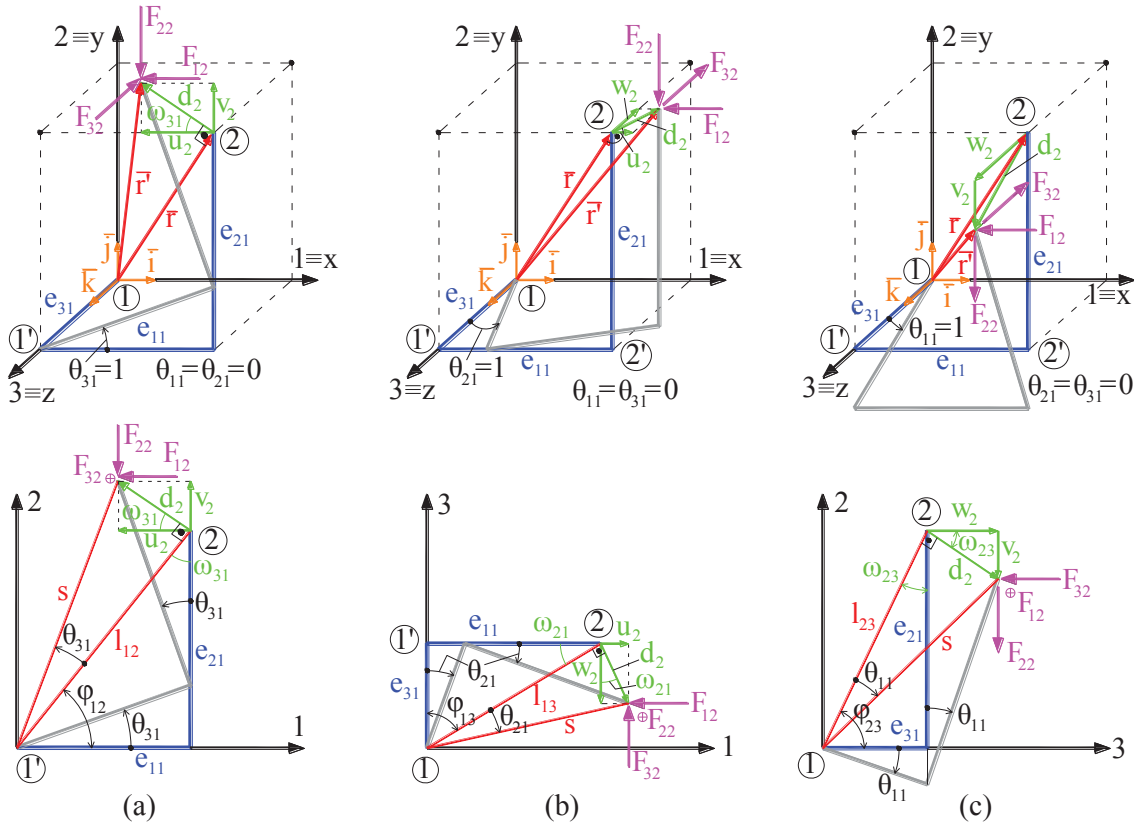

Figure 3: Kinematic conditions of the proposed macroelement's rigid offsets

Due to the fact that the rigid offsets move as rigid bodies in the 3D-space, the displacements of the internal nodes 2 (u_2, v_2, w_2), 3 (u_3, v_3, w_3) are equal to the displacements of the external nodes 1 (u_1, v_1, w_1), 4 (u_4, v_4, w_4) respectively, plus the displacements which are caused by the rotations of the rigid offsets about the local axes 1, 2 and 3 (Figure 3). These additional displacements can be calculated on the basis of Figure 3, with the assumption that the displacements are infinitesimal. Moreover, the behavior of the rigid offsets as absolutely rigid bodies leads to the conclusion that the rotations of the internal nodes 2 (θ_{12}, θ_{22}, θ_{32}), 3 (θ_{13}, θ_{23}, θ_{33}) about the local axes 1,2 and 3 are equal to the corresponding rotations of the external nodes 1 (θ_{11}, θ_{21}, θ_{31}), 4 (θ_{14}, θ_{24}, θ_{34}). It can be proved, with the aid of the Figure 3, that (see also [20]):

$$[u_{int}] = [T] \cdot [u] = \begin{bmatrix} [I_3] & [t_{12}] & [0_3] & [0_3] \\ [0_3] & [I_3] & [0_3] & [0_3] \\ [0_3] & [0_3] & [I_3] & [t_{34}] \\ [0_3] & [0_3] & [0_3] & [I_3] \end{bmatrix} \cdot [u] \quad [t_{12}] = \begin{bmatrix} 0 & e_{31} & -e_{21} \\ -e_{31} & 0 & e_{11} \\ e_{21} & -e_{11} & 0 \end{bmatrix} \quad [t_{34}] = \begin{bmatrix} 0 & e_{32} & -e_{22} \\ -e_{32} & 0 & e_{12} \\ e_{22} & -e_{12} & 0 \end{bmatrix} \quad (11a)$$

$$[u_{int}]^T = [u_2 \ v_2 \ w_2 \ \theta_{12} \ \theta_{22} \ \theta_{32} \vdots u_3 \ v_3 \ w_3 \ \theta_{13} \ \theta_{23} \ \theta_{33}]$$
$$[u]^T = [u_1 \ v_1 \ w_1 \ \theta_{11} \ \theta_{21} \ \theta_{31} \vdots u_4 \ v_4 \ w_4 \ \theta_{14} \ \theta_{24} \ \theta_{34}] \tag{11b}$$

Where $[I_3]$ is the 3x3 identity matrix and $[0_3]$ is the 3x3 zero matrix.

The existence of the rotational springs in the internal nodes 2, 3 causes discontinuity of the rotations about the local axes 2 and 3 in these points. This is expressed through the parameter $\Delta\theta$ and illustrated in Figure 4 for the case of bending of the macroelement in the local plane 1-2, where the rotational springs K_{r32} and K_{r33} are activated.
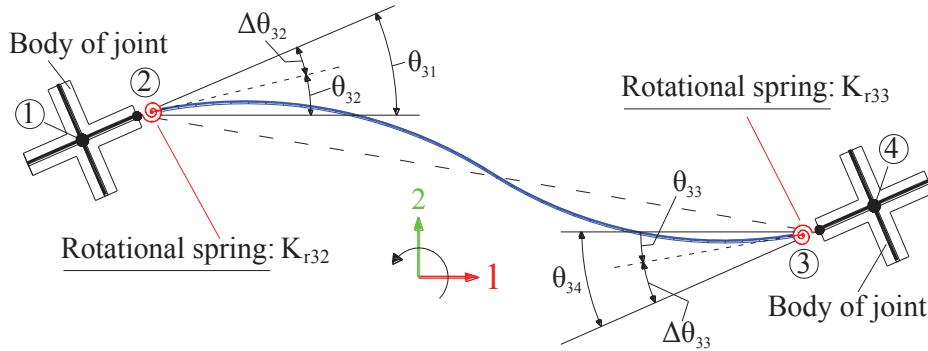

Figure 4: Modelling of semi-rigid connections through the rotational springs in the element's internal nodes

If the rotational springs behave elastically or in the case of inelastic analysis (where, during every incremental step of loading, the tangent stiffness of the rotational springs is used), the equation which gives the value of the discontinuity $\Delta\theta$ is:

$$\Delta\theta_{2i} = M_{2i}/K_{r2i}, \quad \Delta\theta_{3i} = M_{3i}/K_{r3i} \quad (i = 2,3) \tag{12}$$

Thus:

$$\theta_{22} = \theta_{21} - (M_{22}/K_{r22}) = \theta_{21} + (-K_{r22}^{-1}) \cdot M_{22}$$
$$\theta_{23} = \theta_{24} - (M_{23}/K_{r23}) = \theta_{24} + (-K_{r23}^{-1}) \cdot M_{23}$$
$$\theta_{32} = \theta_{31} - (M_{32}/K_{r32}) = \theta_{31} + (-K_{r32}^{-1}) \cdot M_{32}$$
$$\theta_{33} = \theta_{34} - (M_{33}/K_{r33}) = \theta_{34} + (-K_{r33}^{-1}) \cdot M_{33}$$
$$\tag{13}$$

Taking into consideration Eq. (13), Eq. (11a) is modified as follows:

$$[u_{int}] = [T] \cdot [u] + \underbrace{\begin{bmatrix} [0_3] & [0_3] & [0_3] & [0_3] \\ [0_3] & [K_{R2}] & [0_3] & [0_3] \\ [0_3] & [0_3] & [0_3] & [0_3] \\ [0_3] & [0_3] & [0_3] & [K_{R3}] \end{bmatrix}}_{[T_{KR}]} \cdot [S_{int}] \quad [K_{Ri}] = \begin{bmatrix} 0 & 0 & 0 \\ 0 & -K_{r2i}^{-1} & 0 \\ 0 & 0 & -K_{r3i}^{-1} \end{bmatrix} \quad (i=2,3) \tag{14a}$$

$$[S_{int}]^T = \begin{bmatrix} F_{12} & F_{22} & F_{32} & M_{12} & M_{22} & M_{32} \vdots F_{13} & F_{23} & F_{33} & M_{13} & M_{23} & M_{33} \end{bmatrix} \tag{14b}$$

Thus, the matrix equation which relates the displacements of internal nodes 2 and 3 with those of external nodes 1 and 4 is:

$$[u_{int}] = [T] \cdot [u] + [T_{KR}] \cdot [S_{int}] \tag{15}$$

It is also necessary to relate the forces of internal nodes 2 and 3 with those of the external nodes 1 and 4. To this end, the six equations of equilibrium for each one of the two rigid offsets must be formed. These equations state the equilibrium of the three forces and the three moments which act in each one of the two edges of the rigid offsets (nodes 1,2 and nodes 3,4). Obviously, the forces which act at the edges of the rigid offsets are the elements of the vectors [Sint] (Eq. (14b)) and [S], which is the vector of the forces of the external nodes 1, 4:

$$[S]^T = \begin{bmatrix} F_{11} & F_{21} & F_{31} & M_{11} & M_{21} & M_{31} \vdots F_{14} & F_{24} & F_{34} & M_{14} & M_{24} & M_{34} \end{bmatrix} \tag{16}$$

It can be proved [20] that the required relation of the forces of the internal nodes 2 and 3 with those of the external nodes 1 and 4 can be expressed in the following matrix form:

$$[S] = [T]^T \cdot [S_{int}] \tag{17}$$

Eq. (17) arises from the rigid offsets' equilibrium in the undeformed condition of the macroelement. However, in the framework of the geometric non-linear analyses, the equations of equilibrium must be formulated in the element's deformed condition. For this reason, Eq. (17) must be modified. This modification concerns the introduction of the additional moments which are produced when the forces in internal nodes 2, 3 are applied in the deformed state of the element (Figure 3). It can be proved [14] that the modified form of Eq. (17) is:

$$[S] = [T]^T \cdot [S_{int}] + [T_g] \cdot [u] \tag{18}$$

where [u] is the vector of the displacements of the external nodes 1, 4 (Eq. 11(b)) and the matrix $[T_g]$ is calculated by means of the following equation:

$$[T_g] = \begin{bmatrix} [0_3] & [0_3] & [0_3] & [0_3] \\ [0_3] & [K_{s12}] & [0_3] & [0_3] \\ [0_3] & [0_3] & [0_3] & [0_3] \\ [0_3] & [0_3] & [0_3] & [K_{s23}] \end{bmatrix} \quad [K_{sij}] = -\begin{bmatrix} F_{3j}e_{3i}+F_{2j}e_{2i} & 0 & 0 \\ 0 & F_{3j}e_{3i}+F_{1j}e_{1i} & 0 \\ 0 & 0 & F_{2j}e_{2i}+F_{1j}e_{1i} \end{bmatrix} \quad (i,j)=\begin{cases}(1,2)\\(2,3)\end{cases} \tag{19}$$

The relation between the displacements of the internal nodes 2,3 and the external nodes 1,4 (Eq. (15)), as well as the corresponding relation between the forces (Eq. (18)), constitute the basis for the derivation of the stiffness matrix of the macroelement **[kme]** as a matrix function of the stiffness matrix of the macroelement's median segment **[kms]** (Table 1). It can be

proved (e.g. [14]) that, after a sequence of matrix transformations using Eqs. (15), (18), the stiffness matrix **[k_me]** arises from the following equation:

$$[k_{me}] = [T]^T \cdot \left\{ [I_{12}] - [k_{ms}] \cdot [T_{KR}] \right\}^{-1} \cdot [k_{ms}] \cdot [T] + [T_g] \tag{20}$$

where the $[I_{12}]$ is the 12x2 identity matrix.

2.3 Load matrix derivation

The load matrices for the macroelement are formed using the basic principles of the two-step procedure which is used for the derivation of the stiffness matrix. This procedure was described in Section 2.2. The current section focuses on the points of difference between the procedure for the derivation of the load matrices and the corresponding procedure for the derivation of the stiffness matrix.

A) Step 1: Derivation of the load matrix for the median segment

As in case of the derivation of the median segment's stiffness matrix, the corresponding procedure for the formulation of the load matrix is based on the performance of static condensation in two stages (Figure 2). The load matrix of the median segment obviously depends on the shape of the external loading. However, due to the fact that the median segment is discretized in sub-elements, any shape of continuously distributed load can be replaced by concentrated forces which are applied on the generated (**n**-1) nodes and the two external nodes A, B (see Second step in Figure 2). As an example, this procedure for the case of a trapezoidal load on a random part of the median segment is illustrated in Figure 5.
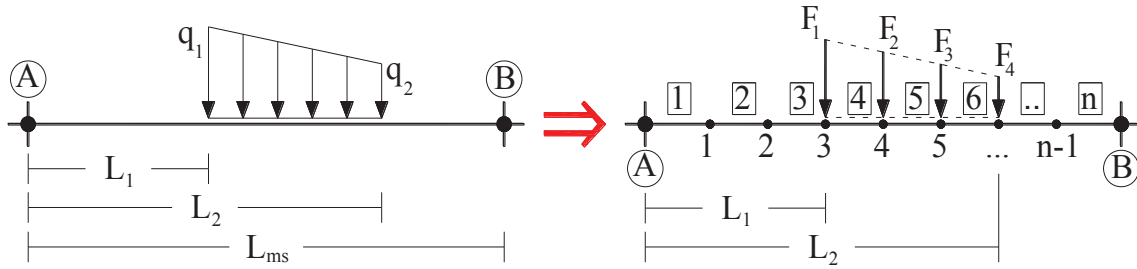

Figure 5: Modelling of distributed load in the median segment through concentrated forces in the generated nodes

Thus, the procedure for the derivation of the load matrix (as is the case with the procedure for the derivation of the stiffness matrix) is based on the consideration of the median segment as a sub-structure which is loaded only by concentrated forces in its nodes. This procedure can generally be programmed, provided that the concentrated forces which replace the actual external load are known. Using this approach, the load matrix **[p_sub]** (Figure 2) is derived. Then, the next steps of the procedure which is illustrated in Figure 2 (third and fourth step) lead to the generation of the 12x1 load matrix **[p_ms]** for the macroelement's median segment.

B) Step 2: Derivation of the load matrix [p_me] for the macroelement

The relation between the displacements and forces of internal nodes 2, 3, considering the external loading of the median segment, is:

$$[S_{int}] = [k_{ms}] \cdot [u_{int}] + [p_{ms}] \tag{21}$$

The corresponding relation for the external nodes 1, 4 is:

$$[S] = [k_{me}] \cdot [u] + [p_{me}] \tag{22}$$

By combining Eqs. (15) and (21), we obtain:

$$[S_{int}] = \{[I_{12}] - [k_{ms}]\cdot[T_{KR}]\}^{-1}\cdot[K_{ms}]\cdot[T]\cdot[u] + \{[I_{12}] - [K_{ms}]\cdot[T_{KR}]\}^{-1}\cdot[p_{ms}] \qquad (23)$$

The combination of Eq. (23) and Eq. (18) leads to the following equation:

$$[S] = \{[T]^T\cdot\{[I] - [k_{ms}]\cdot[T_{KR}]\}^{-1}\cdot[k_{ms}]\cdot[T] + [T_g]\}\cdot[u] + \{[T]^T\cdot\{[I] - [k_{ms}]\cdot[T_{KR}]\}^{-1}\cdot[p_{ms}]\} \qquad (24)$$

Finally, by comparing Eqs. (22) and (24), the load matrix of the macroelement $[p_{me}]$ as a function of the stiffness matrix $[k_{ms}]$ and the load matrix $[p_{ms}]$ of the median segment is extracted:

$$[p_{me}] = [T]^T\cdot\{[I_{12}] - [k_{ms}]\cdot[T_{KR}]\}^{-1}\cdot[p_{ms}] \qquad (25)$$

3 NUMERICAL EXAMPLES

In order to check the efficiency of the proposed macroelement in the geometrically non-linear analyses of framed structures, the solution of a set of numerical examples is presented in the current section. A computer program in Fortran was developed for the implementation of the proposed macroelement in these numerical examples.

3.1 Calculation of the critical load of beam/columns

The ability of the proposed macroelement to accurately calculate the critical loads of beam/columns in lateral buckling was tested using a simply supported beam and a cantilever beam. The data and the boundary conditions of these beams are illustrated in Figure 6. It must be clarified that the ends of both beams are free to warp. Thus, the corresponding bimoments are equal to zero.
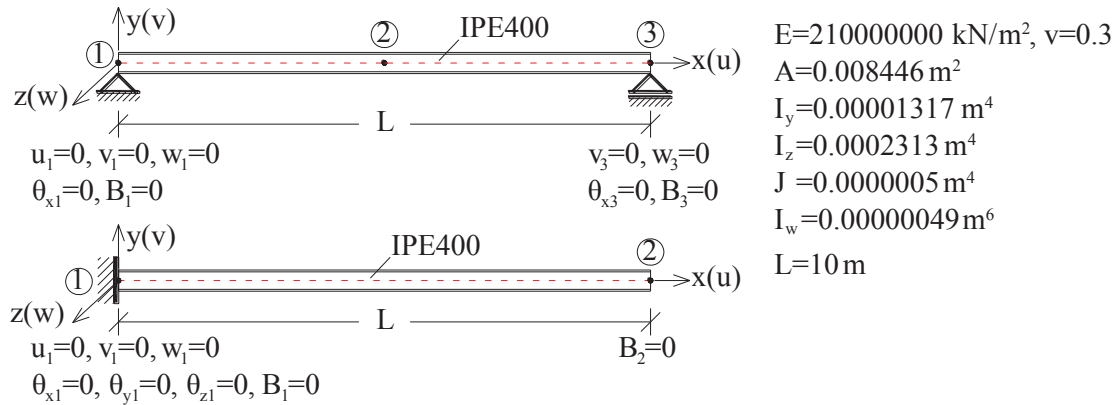

Figure 6: Simple beams for the study of the effectiveness of the new element in the calculation of buckling loads

For the modelling of beams, one macroelement with eight sub-elements was used. Thus, the length of each sub-element is equal to $L_{se}=10/8=1.25$m. The calculated critical load values were compared with the corresponding theoretical ones [21]. Three different load cases for the simply supported beam were considered: (a) pure bending i.e. external moments M_{ze} at its ends, (b) concentrated load F_{ye} at the middle, and (c) uniform load q_{ye}. It must be clarified that the force F_{ye} and the distributed load q_{ye} are applied at the shear center of the beam's cross section. The above load conditions can cause lateral buckling. In order to estimate the critical load in each load case, two different approaches were adopted. In the first approach, the problem was solved by the addition of a perturbation torsional moment M_{xe} at the middle of the beam. The value of this torsional moment was taken equal to 1/1000 of the value of each one

of the three considered external loads. In the framework of this approach, the external loads (and the perturbation torsional moment) were applied incrementally (i.e. step by step). In each load step, the solution was achieved through an iterative procedure. The displacements and the internal forces of the beam were stored after the convergence of each load step. The analyses were terminated when the convergence was impossible, after a pre-defined maximum number of iterations. The termination of analyses indicates the values of the critical loads. In the second approach, the calculation of the critical loads was achieved considering and solving the stability problem. Thus, in each load step (without the perturbation torsional moment M_x), the value of the determinant detK of the stiffness matrix of the restrained beam was calculated and stored. The value of the external load for which the condition detK=0 is fulfilled corresponds to the value of the critical load.
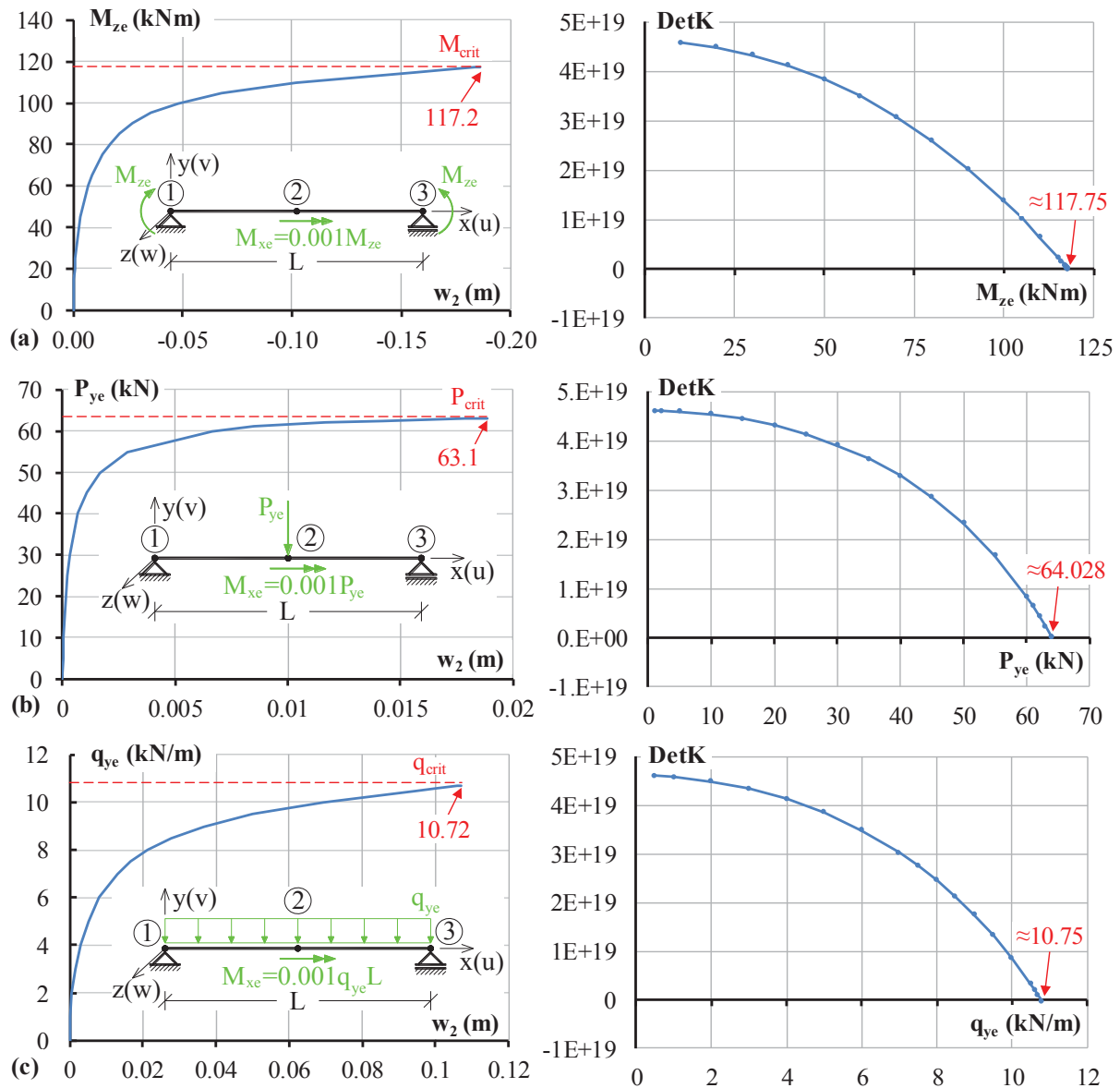

Figure 7: Calculation of critical loads in lateral buckling for a simply supported beam using the new element

Figure 7 illustrates the main results of the analyses described above. The main conclusion to be extracted from this figure is that the implementation of the proposed macroelement can effectively approach the theoretical values of the critical loads for the studied cases (Eqs. (26a)-(26c) [21]). More specifically, the differences of the calculated critical values from the

theoretical ones are 0.47% in the case of the pure bending (Figure 7a), 2.12% in the case of the concentrated load F_{ye} at the middle of the beam (Figure 7b), and 0.34% in the case of the uniform load q_{ye} (Figure 7c) when the first approach is adopted. The differences when the second approach is adopted are correspondingly: 0.01%, 0.68% and 0.06%.

$$M_{cr,L}^{s.s.} = \pi \cdot \sqrt{1 + \frac{EI_w}{GJ} \cdot \frac{\pi^2}{L^2}} \cdot \frac{\sqrt{EI_y GJ}}{L} = 117.76 \text{kNm} \tag{26a}$$

$$P_{cr,L}^{s.s} = 19.239 \cdot \frac{\sqrt{EI_y GJ}}{L^2} = 64.47 \text{kN} \tag{26b}$$

$$q_{cr,L}^{s.s} = 32.1 \cdot \frac{\sqrt{EI_y GJ}}{L^3} = 10.76 \text{ kN/m} \tag{26c}$$

$$P_{cr,L}^{c} = \frac{4.013}{\left[1 - \sqrt{EI_w/(L^2 GJ)}\right]^2} \cdot \frac{\sqrt{EI_y GJ}}{L^2} = 19.04 \text{kN} \tag{26d}$$

Similar conclusions are extracted from the results of the solution of the cantilever beam, which are presented in Figure 8. The theoretical value of the critical load (Eq. (26d), [21]) is effectively approached using both types of analysis procedure. More specifically, the differences between the calculated and the theoretical value of the critical load are 0.72% according to the first approach and 0.59% according to the second one.
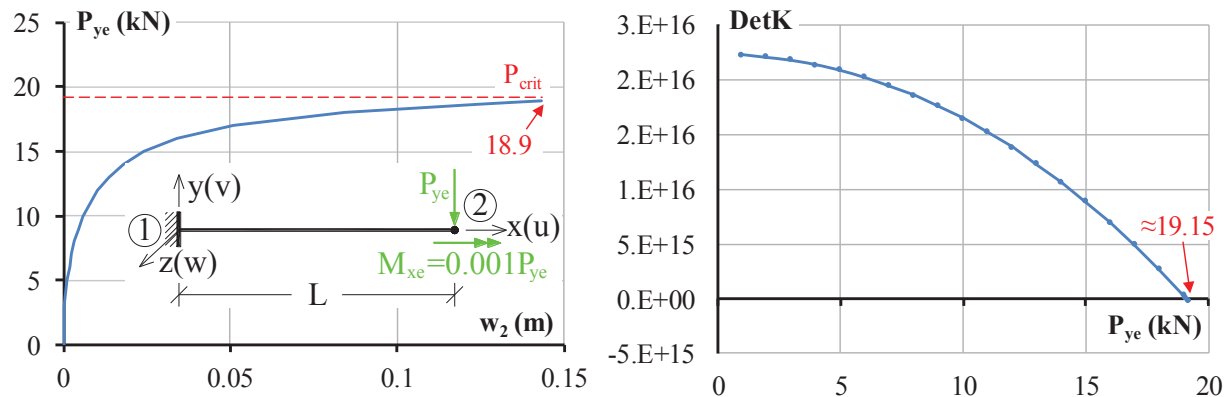

Figure 8: Calculation of the critical load in lateral buckling for cantilever beam using the new macroelement

The efficiency of the proposed macroelement was also studied in the case of an axially loaded column with a cruciform cross-section (Figure 9a). This example was also studied in [22]. The theoretical value of the critical load for pure torsional buckling is available in [21], whereas the corresponding critical value of the axial force for flexural buckling can be calculated by the classic Euler formula. Both of the above critical values of the axial force P_{xe} are given by Eqs. (27a), (27b).

$$P_{cr,t}^{s.s} = \frac{A \cdot GJ}{I_y + I_z} = 195 \text{kN} \tag{27a}$$

$$P_{cr,f}^{s.s} = \frac{\pi^2 \cdot EI_z}{L^2} = 15791.4 \text{kN} \tag{27b}$$

For the solution of the two problems, one macroelement with eight sub-elements was used. The procedure which was adopted for the estimation of the critical axial-torsional buckling load was based on the addition of a perturbation torsional moment M_{xe} equal to 1/1000 of the

applied compressive axial force P_{xe} at the middle of the column (Figure 9b). Correspondingly, a perturbation concentrated force P_{ye} was added for the estimation of the critical axial-flexural buckling load (Figure 9c). As in the case of the beam without an axial force, the external forces were applied progressively (step by step). However, in each one of the loading steps, an iteration procedure was adopted for the accomplishment of the equilibrium between the internal and the external forces. As can be seen in Figure 9, as the compressive axial force approaches the theoretical values of the critical load, the displacements and the rotations at the middle of the column are increased rapidly. In addition, the convergence to the solution became slow. Thus, the algorithm fails to converge after the pre-defined maximum number of iterative steps. The solution with the proposed macroelement gives a value for the critical axial-torsional buckling load that is equal to $P_{cr,t}=194.85$kN (0.08% difference from the theoretical value), whereas the corresponding value for the critical axial-flexural buckling load is 15735kN (0.36% difference from the theoretical value).
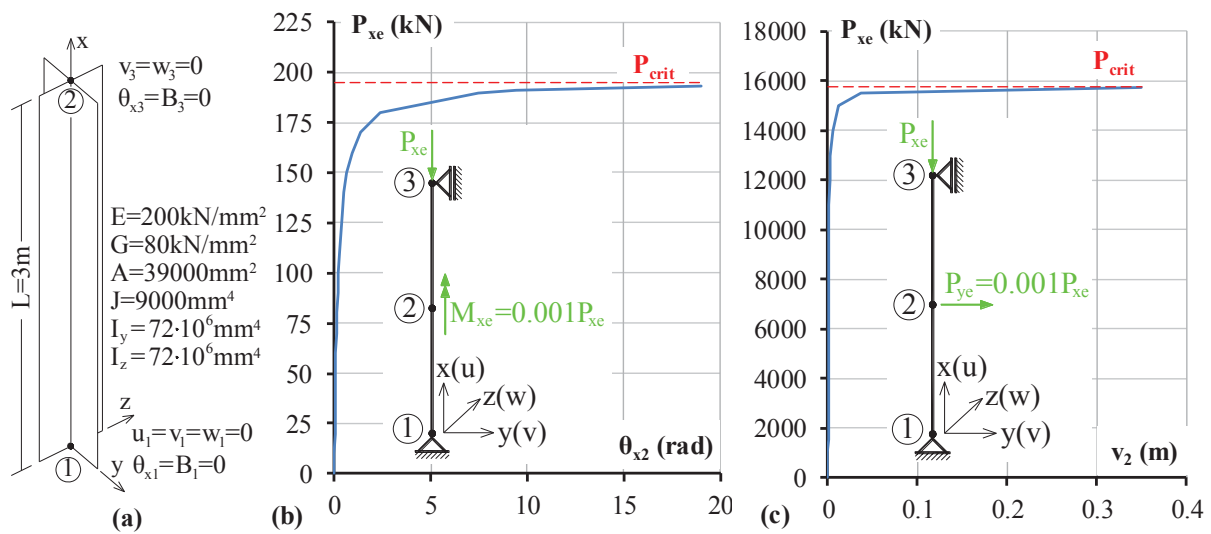

Figure 9: Calculation of critical loads for an axially loaded simply supported column using the new macroelement

3.2 Calculation of the critical load of simple framed structures

The scope of the current section is the study of the performance of the proposed macroelement in the geometric nonlinear analysis of simple framed structures. The extracted results are compared with known solutions or with the corresponding results extracted from reliable software.

The first example of this category is a clamped right-angle frame under a load P at the free end, which was first solved by Argyris et al. [23], as well as by other researchers [22].
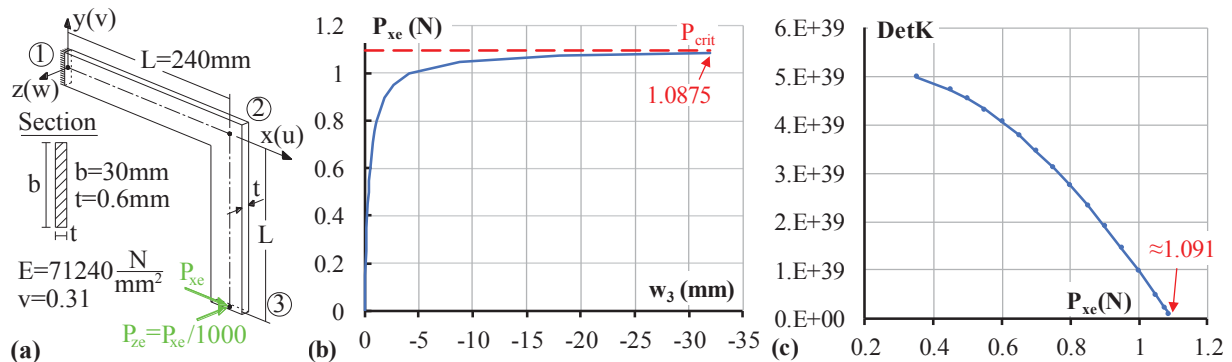

Figure 10: Calculation of the buckling load of a clamped right-angle frame using the new macroelement

The data of this frame are presented in Figure 10. Each one of the two members of the frame was modelled using one macroelement with eight sub-elements.

Following the procedures of the two approaches which were described in the previous section, the values of the frame's critical load were estimated. These values are $P_{cr}=1.0875N$ (first approach) and $P_{cr}=1.091N$ (second approach). The corresponding value which was calculated by Argyris et al. [23], using their formulation for the geometric stiffness matrix and 10 beam elements per member, is $P_{cr}=1.088N$.

The second example of this category concerns the one-storey steel space frame of Figure 11. This example was selected for the study of the performance of the proposed macroelement when its abilities for the modelling of rigid offsets and semi-rigid connections are activated.

Steel: $E_S=2.1\cdot10^8\,kN/m^2$, $v_S=0.3$

Elements 1, 2, 3, 4: IPBv450

Elements 5, 7: IPE400 / Elements 6, 8: IPE450

Rigid offsets: $e_1=0.1535m$, $e_2=0.239m$, $e_3=0.2m$

Semi-rigid connections: $K_{r31}=50000kNm/rad$
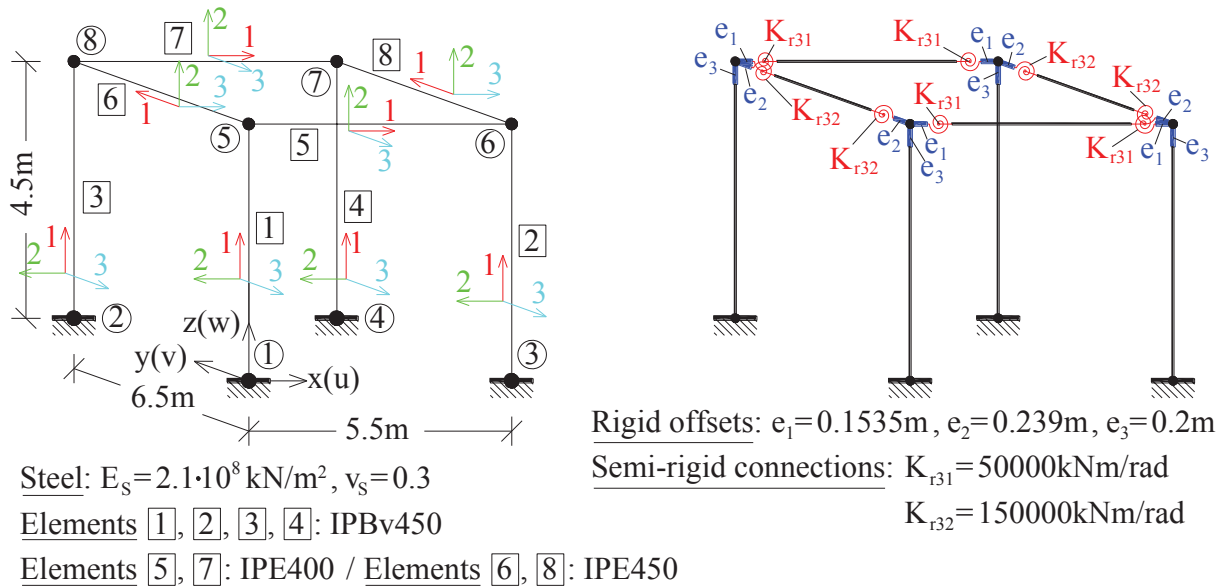
$K_{r32}=150000kNm/rad$

Figure 11: One-storey steel space frame – data and modelling details

Two different types of analyses were performed. The first one concerns the flexural buckling analysis which leads to the calculation of the frame's critical loads. More specifically, the scope of this type of analysis is the calculation of the critical values (eigenvalues) of the load factor λ which correspond to the modes of the overall flexural buckling of the frame for the load pattern of Figure 12. The method which was adopted is based on the estimation of the roots of the equation:

$$\text{Det}\left[K\left(P\cdot\lambda\right)\right]=0 \tag{28}$$

where $K(P\cdot\lambda)$ is the global stiffness matrix of the restrained frame which depends on the external compressive forces P.

These roots were calculated using the Newton-Raphson algorithm. Details for the shape of the function which relates the λ values with the values of $\det[K(P\cdot\lambda)]$ for the examined frame are presented in Figure 12. The first five critical values of factor λ where estimated. Definitely, in practical applications only, the first (and smaller) critical value λ_1 is useful for the design. However, the calculation of the first five critical values of factor λ was carried out for the further study of the effectives of the proposed macroelement.
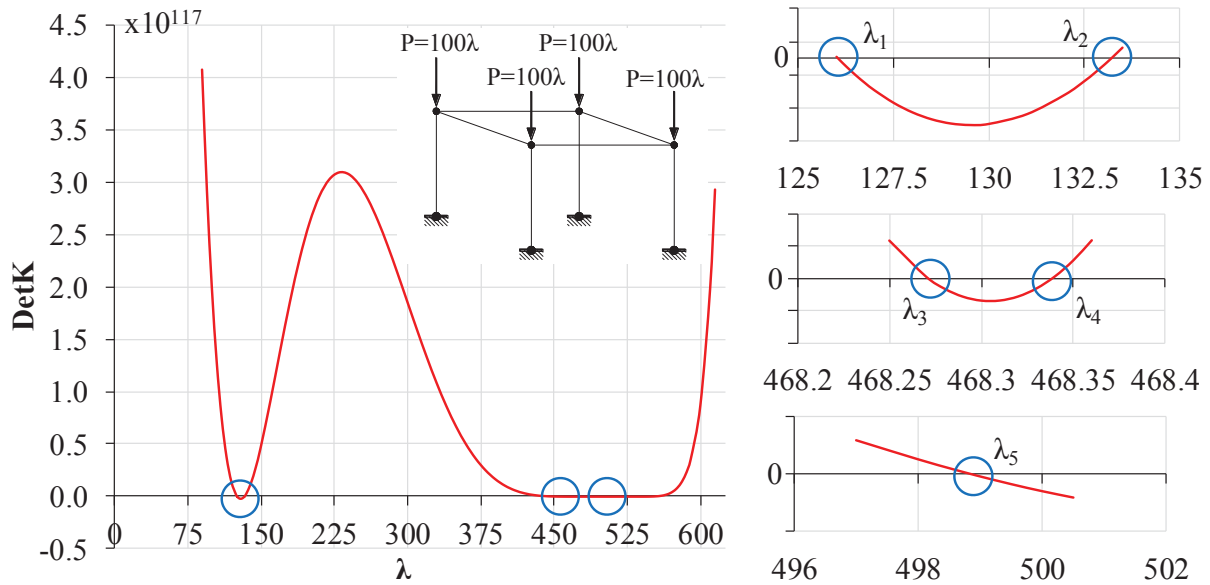
Figure 12: Calculation of the eigenvalues of the overall flexural buckling of the examined space frame using the proposed macroelement

The problem was also solved using the program SAP2000 [24]. Table 2 presents the slight differences of the first five critical λ values between the solution extracted by the SAP2000 program and the corresponding values extracted by the solution using the proposed macro-element.

λ_i	SAP2000	Proposed Macroelement	Difference (%)
λ_1	126.06	126.04	0.014%
λ_2	133.23	133.21	0.019%
λ_3	468.26	468.27	-0.002%
λ_4	468.32	468.34	-0.004%
λ_5	498.86	498.82	0.008%

Table 2: Comparison of the eigenvalues calculated using the new macroelement and the SAP2000 program

The second type of analysis concerns the geometric non-linear analysis of the frame for the vertical (distributed and concentrated) loads and the horizontal concentrated forces which are illustrated in Figure 13.
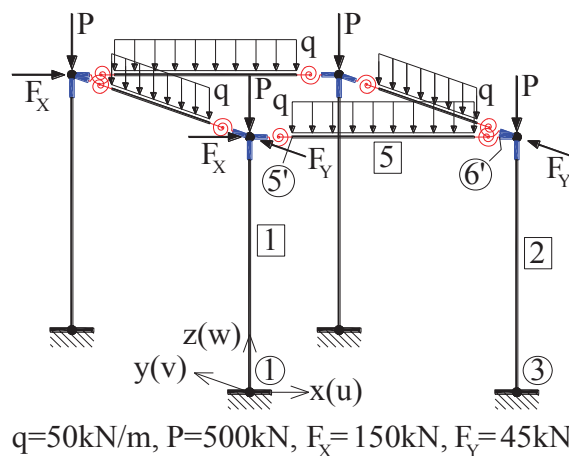

$q=50kN/m$, $P=500kN$, $F_X=150kN$, $F_Y=45kN$

Figure 13: Load case for the geometric non-linear analysis of the space frame

The problem was also solved using the program SAP2000, activating the option for the consideration of the geometric non-linear effects. The comparison between the characteristic results (bending moments and shear forces) which were extracted by SAP2000 and the corresponding results which were extracted by the solution using the proposed macroelement are illustrated in Table 3. This comparison indicates that the proposed macroelement is capable of extracting results very similar to ones extracted by the well-documented SAP2000 program.

Element/Node	Internal Force	Proposed Macroelement	SAP2000	Differences (%)
1/1	$M_{2,1}$	-15.75	-15.72	0.17%
	$M_{3,1}$	178.46	178.37	0.05%
	$V_{2,1}$	-49.40	-49.39	0.02%
	$V_{3,1}$	25.84	25.85	-0.05%
2/3	$M_{2,3}$	-15.82	-15.79	0.22%
	$M_{3,3}$	254.82	254.76	0.02%
	$V_{2,3}$	-100.61	-100.61	0.00%
	$V_{3,3}$	25.85	25.86	-0.03%
5/5'	$M_{3,5'}$	74.33	74.38	-0.07%
	$V_{2,5'}$	78.80	78.75	0.06%
5/6'	$M_{3,6'}$	-190.80	-190.65	0.08%
	$V_{2,6'}$	-180.85	-180.8	0.03%

Table 3: Comparison of values of bending moments and shear forces in characteristic points of the examined space frame using the new macroelement and the SAP2000 program

4 CONCLUSIONS

In the current paper, the formulation and the study of the effectiveness of a proposed beam/column macroelement for non-linear analysis is presented. This macroelement is a two-noded element with seven degrees of freedom per node and possesses abilities to effectively model the members of steel structures. The inclusion of the seventh degree of freedom in each node permits the modelling of the warping effects which are significant in steel members with open thin-walled sections. The proposed formulation is based on a two-stage static condensation technique, which permits the connection of the new element with classic elements with six degrees of freedom per node. The formulation of the new macroelement also includes rotational springs and rigid offsets at ends. It is thus able to model steel members with semi-rigid connections, as well as the influence of the body of rigid joints.

The proposed macroelement was successfully tested using well-known theoretical solutions from the literature and well-documented software (program SAP2000). The macroelement was also inserted to an existing professional software for the analysis and design of steel structures.

REFERENCES

[1] I. Vayas, J. Ermopoulos, G. Ioannidis, *Design of Steel Structures to Eurocodes,* Springer, 2019.

[2] E. Ellobody, R. Feng, B. Young, *Finite Element Analysis and Design of Metal Structures,* Elsevier, 2014.

[3] R. Landolfo, F. Mazzolani, D. Dubina, L.S. da Silva, M. D'Aniello, *Design of Steel Structures for Buildings in Seismic Areas*, *1st Edition*, ECCS, Wiley, 2017.

[4] EN1993-1-1 (Eurocode 3). Design of steel structures - part 1-1: General rules and rules for buildings, European Committee for Standardization; 2005.

[5] ANSI, AISC 360-16, Specification for Structural Steel Buildings; American Institute of Steel Construction: Chi-cago, IL, USA, 2016.

[6] Y.B. Yang, and W. McGuire, Stiffness Matrix for Geometric Nonlinear Analysis, *Journal of Structural Engineering, ASCE*, **Vol. 112, No. ST4**, 853-877, 1986.

[7] Y.B. Yang, and W. McGuire, Joint Rotations and Geometric Nonlinear Analysis, *Journal of Structural Engineering, ASCE*, **Vol. 112, No. ST4**, 879-905, 1986.

[8] S.E. Kim, C.M. Uang, S.H. Choi, and K.Y. An, Practical advanced analysis of steel frames considering lateral torsional buckling, *Thin Wall Struct.*, **44(7)**, 709-720, 2006.

[9] Barsoum RS, Gallagher RH. Finite element analysis of torsional-flexural stability problems, *Int J Numer Methods Eng*, **2**, 335–52, 1970.

[10] E.J. Sapountzakis, V.G. Mokos, 3-D beam element of composite cross-section including warping and shear deformation effect, *Computers and Structures*, **85**, 102-116, 2007.

[11] Y-B Yang, S-R Kuo, *Theory and analysis of nonlinear framed structures*, Prentice Hall, NY, 1994.

[12] *Advanced Analysis of Steel Frames: Theory, Software and Applications*, Ed. W.F. Chen, S. Toma, CRC Press, 1994.

[13] B. Gorenc, R. Tinyou, A. Syam, *Steel Designer's Handbook, 7th edition*, UNSW press, 2005.

[14] K. Morfidis, I.E. Avramidis, Generalized beam-column finite element on two-parameter elastic foundation, *Structural Engineering and Mechanics*, **Vol. 21, No.5**, $519 - 537$, 2005.

[15] K.J. Bathe, *Finite element procedures*, Englewood Cliffs, NJ: Prentice-Hall, 1996.

[16] T.J.R. Hughes, T*he finite element method: Linear static and dynamic finite element analysis*, Prentice-Hall Inc., New Jersey USA, 1987.

[17] E.L. Wilson, The static condensation algorithm, *Int. J. Numer. Meth. Engrg.*, **8**, 198–203, 1974.

[18] Y.B. Yang, and W. McGuire, A Procedure for Analyzing Space Frames with Partial Warping Restraint, *International Journal for Numerical Methods in Engineering*, **Vol. 20, No. 8**, 1377-1398, 1984.

[19] J. Y. R. Liew, H. Chen, N. E. Shanmugam, and W. F. Chen, Improved nonlinear plastic hinge analysis of space frame structures, *Engineering Structures*, **22**, 1324-1338, 2000.

[20] C. S. Krishnamoorthy, *Finite Element Analysis: Theory and Programming*, McGraw Hill, New Delhi, 1995.

[21] S.P. Timoshenko, J.M. Gere, *Theory of Elastic Stability, 2nd edition*, Dover Publications, Inc., 1961.

[22] L.H. Teh, M.J. Clarke, Co-rotational and Lagrangian formulations for elastic three-dimensional beam finite elements. *J Constr Steel Res*, **48(2–3)**, 123–44, 1998.

[23] J.H. Argyris, O. Hilpert, G.A. Malejannakis, D.W. Scharpf, On the geometric stiffness of a beam in space - a consistent V.W. approach, *Comput Methods Appl Mech Eng*, **20(1)**, 105–31, 1979.

[24] SAP2000 Version 21, Integrated finite element analysis and design of structures. Berkeley, California, USA: Computers and Structures Inc.